РІЧКОВИЙ ТА МОРСЬКИЙ ТРАНСПОРТ

UDC 621.436:629.128.6 DOI https://doi.org/10.33082/td.2022.1-12.03

VIBROACOUSTIC DIAGNOSTICS OF MARINE DIESEL ENGINE TURBOCHARGER

R.A. Varbanets[1], O.V. Fomin[2], V.G. Klymenko[3], D.S. Minchev[4], V.P. Malchevsky[5], V.I. Zalozh[6]

[1]DSc, Head of the Department Marine Power Plants and Technical Operation,
Odessa National Maritime University, Odessa, Ukraine,
ORCID ID: 0000-0001-6730-0380

[2]DSc, Professor at the Department of Cars and Carriage Facilities,
State University of Infrastructure and Technologies, Kyiv, Ukraine,
ORCID ID: http://orcid.org/0000-0003-2387-9946

[3]Assistant at the Department of Marine Power Plants and Technical Operation,
Odessa National Maritime University, Odessa, Ukraine

[4]Ph. D., Associate Professor at the Department of Internal Engines,
Installations and Technical Maintenance,
National University of Shipbuilding, Mykolaiv, Ukraine,
ORCID ID: http://orcid.org/0000-0002-5960-3063

[5]Ph. D., Associate Professor at the Department of Marine Power Plants
and Technical Operation,
Odessa National Maritime University, Odessa, Ukraine,
ORCID ID: 0000-0001-6730-0380

[6]Ph. D., Associate Professor at the Department of Engineering Sciences,
Danube Institute of National University "Odessa Maritime Academy",
Izmail, Ukraine,
ORCID ID: https://orcid.org/0000-0002-5213-6896

Summary

Introduction. *Modern turbochargers of marine diesel engines enjoy a high boost pressure ratio in the compressor of up to 5 and above. They create high pressure of the charged air, thus providing high-specific power and high-efficiency operation of the marine engine with low-level emission of carbon oxides and soot. High efficiency of MAN MC and MAN ME diesel engines with actual specific fuel consumption of 160–170 g/kWh is ensured by the high pressure of the charged air, among other factors. In case the turbocharger loses in performance, the power and efficiency of the diesel engine rapidly decline while the emission level of carbon oxides and soot increases. The allowable hazardous emission level of marine diesel engines in operation is limited by the current requirements of the International Maritime Organization. Since the overwhelming majority of various maritime transport vessels use diesel power units, the matter of their efficient and safe operation is undoubtedly of current interest.* ***The article presents*** *the method of vibroacoustic diagnostics of the marine diesel engine turbocharger under operating conditions, when a prompt determination of instantaneous turbocharger speed*

and rotor vibration level is required. The method lies in the analysis of the vibroacoustic signal that is generated by the compressor of the turbocharger with the diesel engine running under load. ***Results.*** *The spectral analysis reveals that the compressor blades generate acoustic oscillations that are always present in the overall vibroacoustic spectrum of the turbocharger regardless of its technical condition. The "blades" harmonic that corresponds to these vibrations can be detected in the spectrum using the method of limits. The calculated instantaneous turbocharger speed makes it possible to analyze the amplitude of the main harmonic in the spectrum. The method presented in the paper helps eliminate the Discrete Fourier Transform (DFT) spectral leakage, so that the amplitude of the main harmonic can be estimated. The further analysis of the amplitude of the main harmonic allows for efficient estimation of the turbocharger rotor vibration level when in operation. The method can be practically applied by the means of a smartphone or a computer that have the dedicated software installed.* ***Conclusions.*** *The proposed method can lay the foundation for the permanent monitoring system of the turbocharger speed and vibration level in the marine diesel engine.*

Key words: *turbocharger diagnostics, marine diesel engine, vibroacoustic spectral analysis, DFT leakage.*

ВІБРОАКУСТИЧНА ДІАГНОСТИКА ТУРБОКОМПРЕСОРА СУДНОВОГО ДИЗЕЛЬНОГО ДВИГУНА

Р.А. Варбанець[1], О.В. Фомін[2], В.Г. Клименко[3], Д.С. Мінчев[4], В.П. Мальчевський[5], В.І. Залож[6]

[1]д. т. н., професор, завідувач кафедри суднових енергетичних установок та технічної експлуатації,
Одеський національний морський університет, Одеса, Україна,
ORCID ID: http://orcid.org/0000-0001-6730-0380

[2]д. т. н., професор кафедри вагонів та вагонного господарства,
Державний університет інфраструктури та технологій, Київ, Україна,
ORCID ID: http://orcid.org/0000-0003-2387-9946

[3]асистент кафедри суднових енергетичних установок та технічної експлуатації,
Одеський національний морський університет, Одеса, Україна.

[4]к. т. н., доцент кафедри двигунів внутрішнього згоряння, установок та технічного обслуговування,
Національний університет кораблебудування імені Адмірала Макарова, Миколаїв, Україна,
ORCID ID: http://orcid.org/0000-0002-5960-3063

[5]к. т. н., доцент кафедри суднових енергетичних установок та технічної експлуатації,
Одеський національний морський університет, Одеса, Україна,
ORCID ID: https://orcid.org/0000-0003-3117-1251

[6]к. т. н., доцент кафедри інженерних дисциплін,
Дунайський інститут Національного університету «Одеська морська академія», Ізмаїл, Україна,
ORCID ID: https://orcid.org/0000-0002-5213-6896

Анотація

Вступ. *Сучасні турбонагнітачі суднових дизельних двигунів мають високий коефіцієнт підвищення тиску в компресорі – до 5 і вище. Вони створюють високий тиск наддувочного повітря, тим самим забезпечуючи високу питому*

потужність і високоефективну роботу суднового двигуна з низьким викидом оксидів вуглецю та сажі. Серед іншого, висока економічність дизельних двигунів MAN MC і MAN ME з фактичною питомою витратою палива на рівні 160–170 г/кВт·год забезпечується високим тиском наддувочного повітря. При зниженні ефективності роботи турбонагнітача, потужність і економічність дизельного двигуна швидко знижуються, а рівень викидів оксидів вуглецю та сажі зростає. Допустимий рівень шкідливих викидів при експлуатації суднових дизельних двигунів обмежений чинними вимогами Міжнародної морської організації. Оскільки переважна більшість морських транспортних суден різного класу має дизельні двигуни, питання їх ефективної та безпечної експлуатації є безумовно актуальним. ***У статті представлено*** *метод віброакустичної діагностики турбокомпресора суднового дизельного двигуна в умовах експлуатації, коли необхідно оперативно визначити миттєву частоту обертання турбокомпресора та рівня вібрації ротора. Метод полягає в аналізі віброакустичного сигналу, який формується компресором турбонагнітача під час роботи дизельного двигуна під навантаженням.* ***Результати.*** *Спектральний аналіз показує, що лопатки компресора генерують коливання, які завжди присутні в спектрі загальної вібрації турбонагнітача незалежно від його технічного стану. «Лопаткова» гармоніка, яка відповідає цим коливанням, в спектрі визначається за допомогою методу обмежень. Розрахована миттєва частота обертання турбокомпресора дозволяє проаналізувати амплітуду основної гармоніки в спектрі. Метод, представлений у статті, допомагає усунути спектральні витоки дискретного перетворення Фур'є (DFT), щоб оцінити амплітуду основної гармоніки. Подальший аналіз амплітуди основної гармоніки дозволяє ефективно оцінити рівень вібрації ротора турбокомпресора під час експлуатації. Метод можна застосувати на практиці за допомогою смартфона або комп'ютера, на якому встановлено спеціальне програмне забезпечення.* ***Висновки.*** *Запропонований метод може бути закладений в основу системи постійного моніторингу частоти і рівня вібрації турбокомпресора суднового дизельного двигуна.*

Ключові слова: *діагностика турбокомпресора, судновий дизельний двигун, віброакустичний спектральний аналіз, виток ДПФ.*

1. Introduction

Modern turbochargers (T/C) of marine diesel engines enjoy a high boost pressure ratio in the compressor of up to 5 and above. They create high pressure of the charged air, thus providing high-specific power and high-efficiency operation of the marine engine with low-level emission of carbon oxides and soot [1]. High efficiency of MAN MC and MAN ME diesel engines with actual specific fuel consumption of 160–170 g/kWh is ensured by the high pressure of the charged air, among other factors [2–3]. In case the turbocharger loses in performance, the power and efficiency of the diesel engine rapidly decline while the emission level of carbon oxides and soot increases [1–3].

The allowable hazardous emission level of marine diesel engines in operation is limited by the current requirements of the International Maritime Organization (IMO) [4]. Since the overwhelming majority of various maritime transport vessels use diesel power units, the matter of their efficient and safe operation is undoubtedly of current interest [5–7].

When a marine diesel engine is operating in light-load conditions, the incomplete combustion products clog up the exhaust manifolds. This results in the change of the flow capacity of the exhaust manifolds as well as the character of the gas internal flow in front of the blades of the turbocharger wheel. Pulsations might occur, which causes the rotor to vibrate [8–10]. Increased level of rotor vibration creates additional loads on turbocharger bearings and reduces their operational life. In case of microdefects in the bearings, the vibration level of the rotor increases even further, which might lead to a severe failure [11].

Vibroacoustic control of the turbocharger in operation makes it possible to detect the dangerous tendency of the vibration level increase of the rotor and indicate the need for cleaning the flow channel [8–11]. In some cases, such control might prevent turbocharger failure, which typically leads to a considerable loss of power and efficiency of the entire engine [1; 11–14].

Many authors have previously pointed out the necessity of conducting operating periodic check of the turbocharger technical condition in operation [11–14]. In such event, prompt and timely diagnostics during operation can be made by analysis of the external vibroacoustic signals. In papers [11; 12] it is indicated that within the spectrum of vibroacoustic oscillations of the turbocharger, regardless of its technical condition, there is always a harmonic present at the "blades frequency" of the compressor wheel. The amplitude of the "blades harmonic" of the compressor considerably exceeds (two, three times or even more) the level of surrounding harmonics in the turbocharger spectrum [8; 12]. Meanwhile, the harmonic of the main rotation frequency of the turbocharger rotor might have insignificant amplitude and might not be distinguishable against the noises of the spectrum [8]. Thus, the "blades harmonic" is the primary source of the turbocharger spectrum analysis and it can be identified in the spectrum using the method of limits.

The paper presents the diagnostic method based on the determination of the "blades" harmonic in the turbocharger spectrum, further calculation of the rotor main speed as well as the subsequent analysis of the harmonic amplitude at its main frequency. The amplitude of the main frequency harmonic characterizes the general vibration level of the turbocharger rotor [5; 6; 15].

The article begins with the analysis of the vibroacoustic signals of the TCA 66 and the VTR 564 turbochargers of low speed diesel engines during their normal operation. The limits of normal and abnormal levels of the amplitude of the main harmonic are illustrated by these two examples. These cases, however, are particular, so it is necessary to analyze the vibroacoustic spectrums of a larger number of turbochargers to develop general recommendations. Nevertheless, we believe that the information will be useful for marine engineers, since these engines are widely used in the merchant marine fleet.

To make the results of analysis more reliable the algorithm of the "leakage effect" eliminating is proposed, which helps to calculate more accurately the frequency and amplitude of the given signal.

A functional diagram of the turbocharger continuous monitoring system is proposed as the general conclusion of the paper.

The method in question can be practically applied; for its realization in most cases, it would suffice to have a smartphone or a personal computer with the dedicated

software. The method lies in the analysis of the vibroacoustic signal that is generated by the turbocharger compressor while the diesel engine is operating under load.

2. TCA 66 turbocharger of low speed diesel engine vibroacoustic analysis

The registration and analysis of vibroacoustic signals of the TCA 66-20072 turbocharger [3], which is installed on the MAN 5S60MC main diesel engine [2], was made at the 85 rpm of engine speed. Estimated engine brake power was ≈4500 kW or 50 % of MCR. According to the sea trials results, the corresponding turbocharger speed should be about 10 300 rpm (see Table 1). The compressor impeller wheel of the TCA66-20072 has 22 blades (11 full blades and 11 splitter blades) [3].

Mechanical engineers provide engine performance analysis during its operation to estimate engine and turbocharger current conditions. The results of performance analysis should be compared with manufacturer's Official Test Data. Among the most important engine parameters for diagnostics are: crank speed and brake power; brake specific fuel consumption; supercharged air pressure; compression pressure and maximum in-cylinder pressure; exhaust gases temperature at the turbocharger inlet and outlet, and turbocharger speed (Table 1).

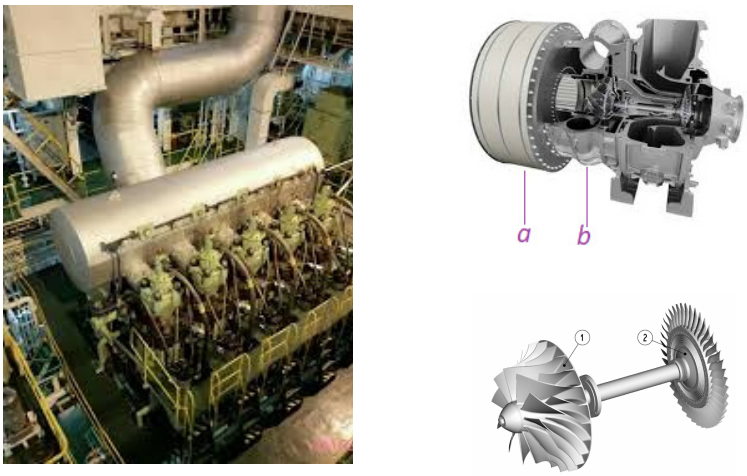

Figure 1. Engine 5S60MC and TCA 66-20072 turbocharger,
1 – compressor wheel, 2 – turbine rotor [3],
(a), (b) – vibroacoustic measuring points

Deviations of these parameters for given engine operating point may be caused by some failures. Thus, for instance, the compression pressure (*P comp*) drop may be caused by cylinder liner wear, piston rings break or sticking, exhaust valve seat leakage/wrong timing or by smaller supercharged air pressure (*P scav*). The reasons of the maximum combustion pressure (*P max*) decrement are generally related to the high-pressure fuel-injection equipment. Smaller exhaust gases temperatures difference at the turbine inlet and outlet (Δ*T/C)* together with turbocharger speed (*T/C rpm)* reduction indicate the flow duct fouling (Table 1).

$$\Delta T/C = T/C\ in - T/C\ out.$$

Suggested method allows the on-going turbocharger speed measuring at engine operation. The compressor vibroacoustic signal registration could be carried out either

at the compressor inlet filter (Figure 1, *a*) or directly at the compressor volute surface (Figure 1, *b*) as it is known from the experiment. The second option (point b) benefits from the inlet flow aerodynamic noise absence.

The aerodynamic noise could also be removed from the recorded signal, if the microphone, (positioned at point a) has the perpendicular orientation to the turbocharger intake filter surface, so the smooth air flow around the microphone is provided. The influence of the noise of other engine mechanisms is relatively small as their sources generally have a big enough distance to the microphone position as it is known from the set of experiments carried out on the number of marine low-speed engines.

Table 1

The main engine 5S60MC Official Test Data

Load, kW	% MCR	Engine RPM	T/C RPM	T/C in t, °C	T/C out t, °C	P scav bar	P max bar	P comp bar	SFOC g/kWh
2208	25	66,1	6150	270	230	0,38	63	43	177,58
4407	49,9	83	9880	300	220	1,06	97,4	66,6	172,99
6621	75	95,4	12050	320	200	1,78	129,8	95	168,16
7937	89,9	101,5	13120	350	210	2,28	139,8	110,2	169,72
8824	99,9	105,3	13850	372	220	2,62	139,8	124	171,13
8820	99,9	105,1	13850	375	220	2,62	139,6	123,8	171,15
9673	109,5	108,2	14540	410	240	2,96	140	136	172,50

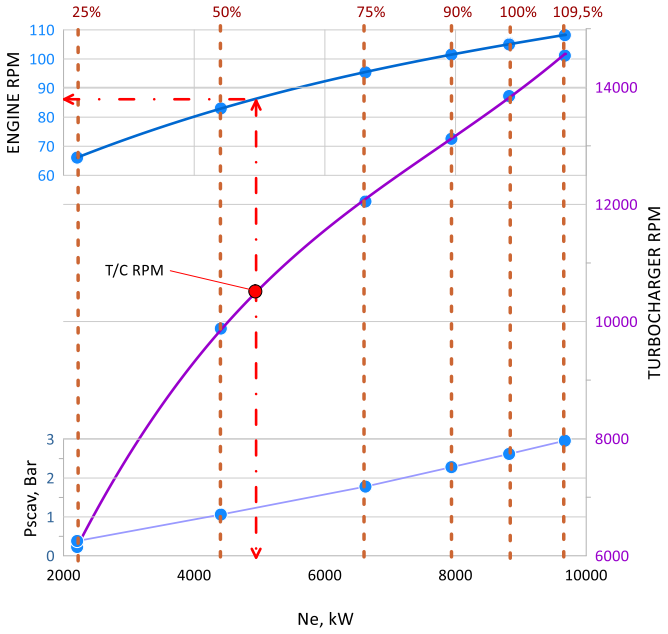

Figure 2. The main engine 5S60MC official test data (engine RPM, Turbocharger RPM, P scav)

According to the Table 1 data, the polynomial equation for the turbocharger speed in respect to the engine brake power was developed (see Table 2). This model can be

applied in practice for fast main engine brake power estimation using the data from vibroacoustic turbocharger analysis. It is valid for known engine and ship hull conditions and for given value of cargo.

Table 2

Polynomial model [5] T/C rpm = f (Ne, kW)

Equation type: **T/C rpm =**	**((Degree3 × Ne + Degree2) × Ne + Degree1) × Ne + Degree0**
Coefficients:	Degree 0 = –25.8849715 Degree 1 = 3.508765178 Degree 2 = –0.0003549392173 Degree 3 = 1.531921627E-08
Model results:	Coefficient of determination, R^2 = 0.999909 Correlation coefficient, R = 0.999954499

The compressor impeller blades generate oscillations in the general spectrum of vibrations regardless of the turbocharger technical conditions as it was experimentally proven [5; 8; 11]. Spectral analysis shows that the vibroacoustic signal from the compressor blades has the frequency equal to the turbocharger rotor speed multiplied by the blades number (see Figure 3):

$$\upsilon_b = n_b \times \text{T/C rpm} / 60 \quad (1)$$

were υ_b – blades frequency of the turbocharger, Hz; n_b – total number of compressor wheel blades; T/C rpm – turbocharger speed, rpm.

Assuming that current engine operating point is between 100 % and 25 % of MCR, so the top and bottom limits for turbocharger speed could be estimated (for MAN 5S60MC engine):

- Max blade frequency ($\upsilon_{b\ max}$) = n_b × max T/C rpm / 60 = 22 blades × 13850 rpm / 60 = 5078 Hz,
- Min blade frequency ($\upsilon_{b\ min}$) = nb × min T/C rpm / 60 = 22 blades × × 6150 rpm / 60 = 2255 Hz.

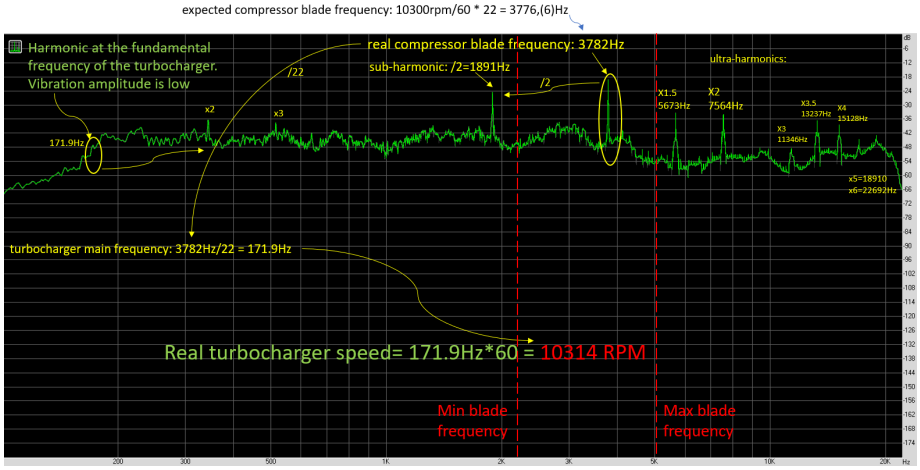

Figure 3. The spectrum of the vibroacoustic signal of the compressor of the TCA 66-20072 turbocharger at 50 % load mode of the engine 5S60MC (4500 kW, 85 rpm)

Thus, the “blades” harmonic in the general turbocharger spectrum lies between these limits (Figure 3):

$$\upsilon_{b\,min} < \upsilon_b < \upsilon_{b\,max}.$$

The experimental measurements (Figure 4) were made with the electret microphone EM-4015-BC produced by Soberton Inc. [16]. The microphone has high sensitivity, wide pass band, narrow directional pattern, small distortion and low noise level. It should be noted, that due to the current microphone upper limit the presented spectrum above 12 kHz could be incorrect, but it isn’t significant as for the low-speed diesel engines turbochargers it isn’t necessary to record the signal over 10 kHz, so it doesn’t affect the conclusion.

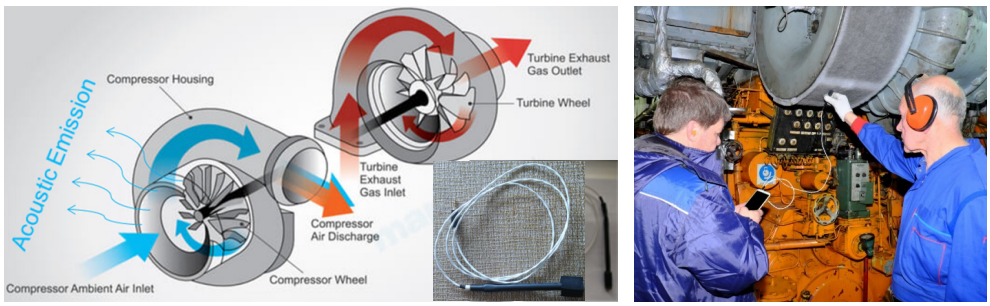

Figure 4. Recording the vibration of turbocharger using the EM-4015-BC electret microphone

The spectrum analysis (from Figure 3) reveals the value of actual blades frequency: 3782 Hz. Thus, the actual turbocharger speed equals to: 3782 Hz / 60 = 171.9 Hz. So, for a given engine operating point the TCA 66-20072 turbocharger actual speed is equal to: 171.9 Hz × 60 = 10314.5 rpm.

It is notable that the main frequency (171,9 Hz) harmonic amplitude is relatively small and could be estimated at the range of spectrum noise. This could be assumed as the indication of small turbocharger rotor vibrations level and highly probable as the indication of the rotor bearings normal conditions [8; 12].

Vibroacoustic spectrum of TCA 66-20072 turbocharger also has sub-harmonics and ultra-harmonics:

- sub-harmonic x0.5 = 1891 Hz;
- ultra-harmonics x2 = 7564 Hz, x3 = 11346 Hz, x4 = 15128 Hz, x5 = 18910 Hz, x6 = 22692 Hz.

Sub-harmonics and ultra-harmonics could be used as additional diagnostic signs for further experimental measurements of turbocharger operation.

For the signal, recorded at 44.1 kHz of frequency it is possible to make spectrum analysis for harmonics with frequency up to 22.05 kHz [17]. For the most marine engines the “blades” frequency of turbocharger is always at least 2 times smaller. Maximum frequency of recorded signal is also limited by the microphone characteristics. As the possible step for spectrum analysis is down to 1 Hz, the absolute error of turbocharger frequency estimation is generally <1 rpm. The measurement time should be related to the response time of a turbocharger, which is typically about 1 to 3 s. So, the accuracy

of suggested method for turbocharger frequency measurement exceeds the typical accuracy of standard measuring devices.

Suggested method could be used for accurate measurements of instantaneous turbocharger speed, turbocharger rotor vibrations level estimation and for rough estimation of the engine brake power.

3. VTR 564 turbocharger of low speed diesel engine vibroacoustic analysis

Another set of experimental research was carried out for ABB VTR 564-31 turbocharger [18], installed of the MAN 6L80MCE main marine engine of the capsize bulker [19]

The compressor impeller has 20 blades and its vibroacoustic spectrum for the engine operating point close to MCR is shown in Figure 5. The assumed value of turbocharger speed for such conditions should be smaller than the turbocharger speed at the engine rated power. So, the turbocharger speed for MCR operated point could serve as the top limit.

$$\text{Max blade frequency } (\upsilon b \text{ max}) = nb \times \text{max T/C rpm} / 60 =$$
$$= 20 \text{ blades} \times 9000 \text{ rpm} / 60 = 3000 \text{ Hz}.$$

As the engine operating point could be estimated as close to MCR or at least between 50 % and 100 % of MCR, the bottom limit of the turbocharger speed could be assumed as (υ_b min) = 1500 Hz.

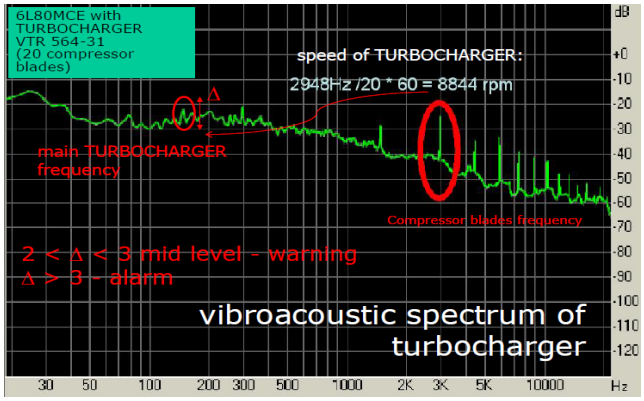

Figure 5. Recording the vibration of turbocharger using the EM-4015-BC electret microphone

By scaling the spectrum diagram (Figure 5) the value of "blades" frequency was estimated as 2948 Hz – it is the closest harmonic to the top limit of 3 kHz. The left harmonic in the diagram (respect to the "blades" harmonic) is the sub-harmonic which has a two times smaller frequency – 1474 Hz.

From the "blades" turbocharger frequency the turbocharger rotor speed was calculated as:

$$\text{RPM turbocharger} = 60 \times 2948 \text{ Hz} / 20 = 8844 \text{ rpm}.$$

The turbocharger standard tachometer was indicating the turbocharger speed as 8800 rpm, so the error of the turbocharger speed estimation is about 0.5 %. It is important to underline: as the error of turbocharger speed estimation by vibroacoustic method is generally less than 1 rpm it provides much more accurate turbocharger speed and further engine operating point estimation.

The frequency of the main harmonic for the turbocharger rotor speed is:

$$\upsilon \text{ turbocharger} = \upsilon b / nb = 2948 \text{ Hz} / 20 = 147{,}4 \text{ Hz}.$$

Obviously, the relatively high level of the main harmonic amplitude Δ could be an indication of increased level of rotor vibrations [8]. The level of main harmonic amplitude Δ in Figure 5 could be assumed as lightly increased but still permissible.

In all cases of measurements on marine engines, when high levels of fundamental harmonics were found, it was necessary to clean the flow path of the turbochargers. After cleaning, the level of the fundamental harmonic decreased down to $\Delta < 2$.

The set of experiments carried out on the number of MAN MC-series diesel engines has shown that if the main harmonic amplitude becomes 2–3 times greater than the spectrum average level it indicated the dangerous level of turbocharger rotor vibrations [12]. The average spectrum amplitude level was estimated in a range of:

$$[\upsilon \text{ turbocharger} - 50 \text{ Hz} \div \upsilon \text{ turbocharger} + 50 \text{ Hz}].$$

More precise quantitative assessment of the permissible range of turbocharger rotor vibrations level requires further experimental investigations. It is important to accentuate the ability to make such an assessment rapidly during engine normal operation and without any additional devices installation on the engine.

4. Eliminating the "leakage effect" of discrete spectrum (LEE)

In the process of analyzing the discrete spectrum of vibroacoustic signals in order to estimate their frequency and amplitude characteristics, it is necessary to solve the problem of eliminating the effect of "leakage". This effect is a consequence of the finiteness of the analyzed temporal realization and its discrete representation. The effect of "leakage" or outflow of power from the spectral peaks into the adjacent spectral lines is considered to be one of the main DFT errors [17].

As an example, Figure 6 shows the amplitude spectra of the same sinusoidal signal with an integer (a) and a non-integer (b) number of samples per one signal period.

Let the frequency of a signal be represented by

$$\gamma = M/T,$$

where T is the period of the signal; $M = n + \sigma$, where n is an integer and $0 < \sigma < 1$.

The maximum distortions of the amplitude, frequency and phase of the central harmonica and leakage of power into the neighboring ones will be observed at $\sigma = 0{,}5$ [17].

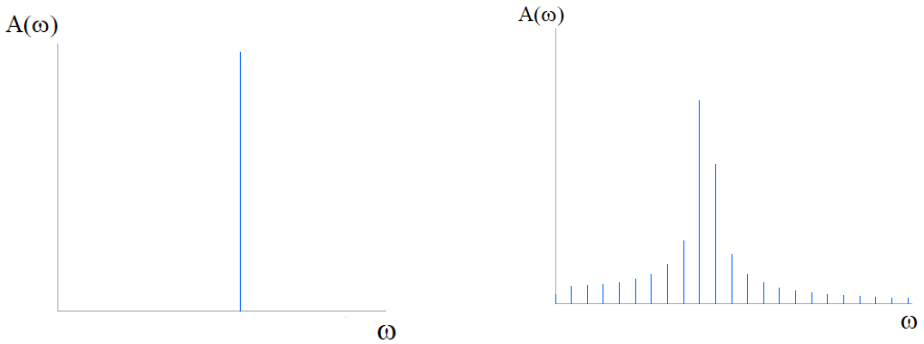

(a) σ = 0 **(b) σ ≠ 0**

Figure 6. The DFT leakage effect.
Integer (a) and a non-integer (b) number of samples per period

Thus, when analyzing the parameters of the original spectrum signal, i. e. the central harmonic, the resulting amplitude, frequency and phase will be distorted in case of a non-integer number of signal samples per its period. In practice, for discrete recording of signals, an Analog to Digital Converter (ADC) with a selected and fixed sampling rate is used. It is understandable that the number of samples per period will never be an integer and the value of σ will change from 0 to 1 depending on the natural frequency of the measured signal, and the accuracy of estimating the signal parameters along the central harmonic will change.

The most common solution for leakage effect reduction is based on window transform methods. The essence of the method is simple: to reduce the number of discontinuities at the edges in order to reduce leakage it is necessary to reduce the amplitude of the signal near the edges. This scaling is carried out during the implementation of the multiplication by the window with the special form $s_j^w = s_j \cdot W(j)$, where *W(j)* is stands for Window functions, Table 3.

As a result of applying window functions, the spectrum of the original signal is changed and its amplitude decreases by RMS Coeff times, as shown in Table 3. Thus, the dependence of the amplitude of the fundamental harmonic in the spectrum from the value of σ decreases. This means that the fundamental harmonic can be used to approximate the signal parameters with a certain constant error, which can be taken into account.

Table 3

Window functions used to reduce the DFT "leakage effect" [17]

window	RMS Coeff	equation
Hemming	1,414	$\varpi(n) = 0,53836 - 0,46164\ \cos\left(\frac{2\pi n}{N-1}\right)$
Hanning	1,633	$\varpi(n) = 0,5\ \left(1 - \cos\left(\frac{2\pi n}{N-1}\right)\right)$
Kaiser	1,61	$\varpi(n) = \frac{\left\lvert I_0\left(\beta\sqrt{1-\left(\frac{2n-N+1}{N-1}\right)^2}\right)\right\rvert}{\lvert I_0(\beta)\rvert}$
Blackman-Harris	1,585	$\varpi(n) = 0,42 - 0,5\cos(2\pi n / (N-1)) + 0,8\cos(4\pi n / (N-1))$

More precisely, we can eliminate the "leakage effect" by a numerical method based on the processing of the complex DFT results. In [17], a suggestion was made that the frequency m, the phase φ, and the amplitude A of the original signal from the values of two maximum harmonics in the spectrum should be specified. For this it is proposed to solve numerically the system of complex equations. To do so, the system of complex equations is proposed to be solved numerically:

$$\left\{\begin{array}{l} \left|E(m,\phi)_k \ / \ E(m,\phi)_{k+1}\right| = \left|X_k \ / \ X_{k+1}\right| \\ \mathrm{Arg}(E(m,\phi)_k) = \mathrm{Arg}(X_k) \end{array}\right\}, \quad (2)$$

where the parameters of the k-th harmonic are specified as: $X_k = \mathrm{Re}_k + j\,\mathrm{Im}_k$,

$$X_k = NA_k e^{j\phi_k},\ A_k = \frac{1}{N}\sqrt{\mathrm{Re}^2{}_k + \mathrm{Im}^2{}_k},\ \phi_k = \mathrm{arctg}(\frac{\mathrm{Im}_k}{\mathrm{Re}_k}) = \mathrm{Arg}(X_k).$$

The harmonic coefficients can be represented in the form: $X_k = (A_k / 2)E(m,\phi)_k$, where $E(m,\phi)_k$ is a complex function independent of the amplitude, but dependent on the frequency and phase:

$$E(m,\phi)_k = e^{j\phi}\frac{e^{2\pi j(m-k)} - 1}{e^{\frac{2\pi j(m-k)}{N}} - 1} + e^{-j\phi}\frac{e^{-2\pi j(m+k)} - 1}{e^{\frac{-2\pi j(m+k)}{N}} - 1}. \quad (3)$$

The system of equations (2) must be solved in the case where the harmonics to the left and right of the central one are not equal to zero (in practice it is more than a given small value δ):

$$X_{k-1} > \delta, X_{k+1} > \delta.$$

If $X_{k-1} = 0,\ X_{k+1} = 0$, then the leakage effect is absent and the frequency, amplitude and phase of the central harmonica correspond to parameters of the measured initial signal (Figure 6a).

When solving the system (2) for the situation of strong leakage effects (σ ~ 0,5), only five full iterations were required to provide a specified error of less than 0.5 % in frequency and phase. For a sinusoidal signal, the amplitude and frequency are recovered to the value specified in the original signal with accuracy to 5 decimal places. In this case, the amplitude of the central harmonic in the spectrum after the DFT before the recovery procedure was with an error of 35 % (!) [12; 17].

An error in estimating the frequency of the original signal with respect to the frequency of the central harmonic can also be significant. It depends on the frequency of the ADC and the frequency of the original signal. As the frequency of the ADC increases, it will decrease.

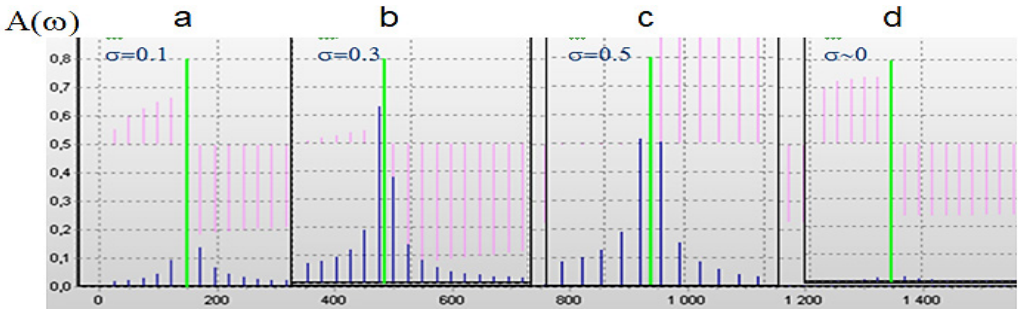

Figure 7. DFT leakage effect eliminating [12; 17]

The solution of the system (2) is not associated with additional memory as is the case for the fast Fourier transform (FFT). Despite the iterative numerical solution for system (2), such procedure only very slightly increases the overall computation time, and make it possible to obtain not only the spectrum of the signal, but also the restored value of the fundamental frequency, amplitude and phase of the measured signal, when it is close to sinusoidal.

This method was investigated in case of noise in the original signal (with a white noise of 5 % and 10 % of the amplitude of the sinusoid). Figure 7 shows the solution

of the system (2) for a sinusoid with an amplitude of 0,8 and for the cases a) σ = 0,1, b) σ = 0,3 c) σ = 0,5 and c) σ = 0.

The central green line in each Figure 7 a, b, c, d is the main harmonic of a sinusoid with amplitude of 0,8 with the restored amplitude, frequency and phase, being a result of solving the system of equations (2).

For all the cases, not more than 5 complete iterations were required to ensure a given accuracy. As a result of the solution of the system (2), the phase and frequency of the signal with the addition of white noise to 10 %, are restored to the initial value with an error of not more than 0.5 %.

5. Conclusions

The proposed method allows to determine the turbocharger rotor speed and level of the vibration by means of stabilizing harmonics amplitude of vibroacoustic spectrum using proposed algorithm. The method can be implemented in the continuous monitoring system of the turbocharger, Figure 8.

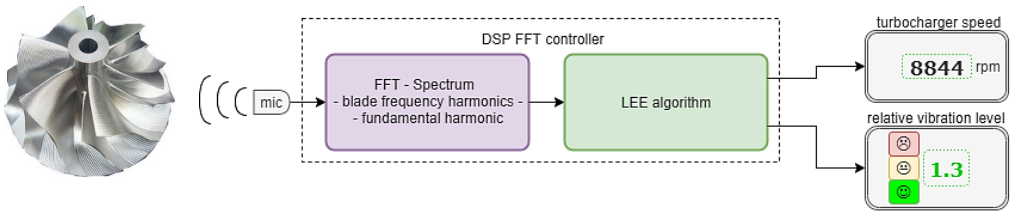

Figure 8. Block diagram of a turbocharger vibroacoustic continuous monitoring system

In accordance with the main directions of increasing the efficiency of vehicles [20], it is relevant to reduce operating costs by eliminating undesirable effects and using more technologically advanced and practical equipment. Tests on two-stroke marine engines have shown that a mobile version of a smartphone-based vibroacoustic measuring system can be realized.

Expected features of the proposed system:

- continuous monitoring of turbocharger rotation speed and rotor vibration level;
- reliability and ease of installation, as the sensor is in a low temperature zone;
- high accuracy rotation speed control, which makes it possible to monitor the total engine load.

In order to define the limits of normal and abnormal rotor vibration levels for various types of turbochargers, further research is necessary. It may be noted that the vibroacoustic spectrum analysis of turbocharger can be quickly made under the operating conditions and does not require significant expenses.

Author Contributions: Conceptualization, R. V. and V. K.; methodology, R. V., O. F. and V. K.; software, R. V., V. K. and D. M.; validation, A. K. and V. Z., writing, review and editing, A. K. and V. K. All authors have read and agreed to the published version of the manuscript.

Acknowledgments: The authors thank to Odessa National Maritime University and National University of Shipbuilding, Mykolaiv for support.

The authors thank the IMES GmbH company for providing the data sets employed in this work.

Conflicts of Interest: The authors declare no conflicts of interest.

Abbreviations

The following abbreviations are used in this manuscript:

T/C	Turbocharger
MAN MC	This type of MAN engines uses a mechanically driven camshaft for fuel injection, cylinder lubrication, and to control the timing of the starting air and exhaust
MAN ME	Electronically controlled engines
MCR	Maximum continuous rating is defined as the maximum output that an engine is capable to produce continuously under normal conditions
DFT	Discrete Fourier transform
FFT	Fast Fourier transform
LEE	DFT leakage effect eliminating
ADC	Analog to Digital Converter
RMS	Root mean square
IMO	International Maritime Organization

REFERENCES

1. Heywood, B. Internal Combustion Engine Fundamentals. New York; London : McGraw-Hill Education, 2018.
2. MAN B&W S60MC-C8.2-TII Project Guide. Available online: https://marine.man-es.com/applications/projectguides/2stroke/content/printed/S60MC-C8_2.pdf (accessed on 5 November 2020).
3. TCA Turbocharger Project Guide. Available online: https://turbocharger.mandieselturbo.com/docs/default-source/shopwaredocuments/tca.%20pdf?sfvrsn=2 (accessed on 5 November 2020).
4. Čampara, L., Hasanspahić, N., & Vujicic, S. (2018). Overview of MARPOL ANNEX VI regulations for prevention of air pollution from marine diesel engines. SHS Web of Conferences. 58. 01004. 10.1051/shsconf/20185801004.
5. Varbanets, R., & Karianskiy, A. (2012). Marine diesel engine performance analyze. Journal of Polish CIMAC. Energetic Aspects. Gdansk: Faculty of Ocean Engineering and Ship Technology Gdansk University of Technology, 7 (1), 269–275.
6. Fomin, O., Lovska, A., Píštěk, V., & Kučera, P. (2019). Dynamic load computational modelling of containers placed on a flat wagon at railroad ferry transportation. VIBROENGINEERING PROCEDIA 2019, Greater Noida (Delhi), India, 118–123, doi: 10.21595/vp.2019.21132
7. Fomin, O., Lovska, A., Píštěk, V., & Kučera, P. (2020). Research of stability of containers in the combined trains during transportation by railroad ferry. MM SCIENCE JOURNAL, 3728–3733.
8. Solomatin, S. Foundations of technical diagnostics. Odessa, ONMU, 2007, 80 p.

9. Píštěk, V., Kučera, P., Fomin, O., & Lovska, A. (2020). Effective Mistuning Identification Method of Integrated Bladed Discs of Marine Engine Turbochargers. J. Mar. Sci. Eng. 8, 379.
10. Píštěk, V., Kučera, P., Fomin, O., Lovska, A., & Prokop, A. (2020). Acoustic Identification of Turbocharger Impeller Mistuning – A New Tool for Low Emission Engine Development. Appl. Sci., 10, 6394.
11. Zigelman, E., Skvortzov, D., & Loshinin, I. (2013). Study of Possibility for vibrodiagnostics of medium diesel generators. Izvestiya vuzov, 6, 42–48.
12. Varbanets, R., & Kucherenko, Y. (2013). Turbocharged Marine diesel engine frequency parameters monitoring. Bulletin of the Astrakhan State Technical University. Series: Marine equipment and technology. 1, 103–110.
13. Kostyukov, V., & Naumenko, A. (2009). Condition monitoring of reciprocating machines. – In: COMADEM 2009, 22nd Intern. Congress of Condition Monitoring and Diagnostic Engineering Management. San Sebastian (Spain): Fundacion TEKNIER, 113–120.
14. Naumenko, A. (2009). Real-time condition monitoring of reciprocating machines. In: The 6th Intern. Conf. on Condition Monitoring and Machinery Failure Prevention Technologies. Dublin (Ireland), 1202–1213.
15. ISO 10816 Series. Mechanical vibration: Evaluation of machine vibration by measurements on non-rotating parts.
16. EM-4015-BC, Analog Microphone Electret Condenser 1V~10V Omnidirectional (–44 dB ±3 dB @94 dB SPL) Solder Pads. Available online: https://www.soberton.com/em-4015-bc/ (accessed on 5 November 2020).
17. Otnes, R., & Enochson, L. Applied Time Series Analysis, by New York: Wiley, 1978, 428 p.
18. VTR564E32 ABB Turbo Systems. Available online: https://library.e.abb.com/public/18a4237f8f5b406e9a9a92aa74aeb501/ZTL2104.pdf (accessed on 5 November 2020).
19. Hanjin Dampier. Available online: https://www.atsb.gov.au/media/24941/mair184_001.pdf (accessed on 5 November 2020).
20. Fomin, O. V. (2015). Increase of the freight wagons ideality degree and prognostication of their evolution stages. Scientific Bulletin of National Mining University, 3, 68–76. http://nv.nmu.org.ua/index.php/en/monographs-and-innovations/monographs/1078-engcat/archive/2015/contents-no-3-2015/geotechnical-and-mining-mechanical-engineering-machine-building/3040-increase-of-the-freight-wagons-ideality-degree-and-prognostication-of-their-evolution-stages